International Journal of Machine Tools & Manufacture 92 (2015) 41–51

Contents lists available at ScienceDirect

International Journal of Machine Tools & Manufacture

journal homepage: www.elsevier.com/locate/ijmactool

A new geometric error modeling approach for multi-axis system based on stream of variation theory

Hao Tang [a,b,1], Ji-an Duan [a,*], Shuhuai Lan [b], Huanyi Shui [b]

[a] State Key Laboratory of High-performance Complex Manufacture, Central South University, Changsha, Hunan 410083, China
[b] S.M. Wu Manufacture Center, University of Michigan, Ann Arbor, MI 48109, USA

ARTICLE INFO

Article history:
Received 20 November 2014
Received in revised form
5 February 2015
Accepted 27 February 2015

Keywords:
Geometric error modeling
Multi-axis system
Stream of variation
Error propagation
Multi-axis precision stage

ABSTRACT

This paper introduces a new geometric error modeling approach for multi axes system (MAS) based on stream of variation (SOV) theory, especially for multi-axis precision stage. SOV is used for measuring product quality for some complicated multi operations system, which is widely used in error propagation in engineering field. This paper introduces SOV concept into geometric error modeling for MAS. Instead of different process in manufacture, the new error modeling approach regards each axis as a station in MAS, and calculates the deviations after each station which is considered as upstream factor to next station. It is clear to observe how geometric errors give influence and how deviations accumulate. Different with conventional methods which are only used for error compensation in machine tools, the new error model is beneficial for sensitive error control and optimal configuration selection in design part. In addition, the new error modeling has some merits such as debugging easily due to observe the deviations after every station. A case study of new error modeling procedure for six-axis stage (SAS) in optoelectronic packaging system (OPS) is developed, and applications related to error reduction order and optimal configuration selection are processed based on the new error model.

1. Introduction

Multi axes system (MAS), such as multi-axis machine tool and manipulators in high accuracy control, or aerospace engineering for specific positioning tasks, plays an essential role in many regions. There are several kinds of errors in MAS that contributes on deviations, including geometric error, thermal error and servo error etc. Among these errors, geometric error gives great impact on pose accuracy [1–3]. In order to achieve high accuracy in MAS, a comprehensive error model is necessary so that deviations can be predicted. For five-axis machine, the geometric error model is used to calculate the deviations of tool tip, so the application for error model is only adopted in error compensation in most cases. However, another kind of typical MAS, multi-axis precision stage (MPS) is widely utilized in engineering regions such as in optoelectronic packaging system (OPS). Because of small scale and good environment, other errors are overwhelmed by geometric errors in most cases in MPS. Conventional error modeling method only knows the deviation of one object fixed on MPS in final step but cannot reveal how geometric error gives impact and how error propagates in the whole procedure. Considering that current error modeling approach is not suitable for many applications, a systematic and comprehensive error modeling method is required for MPS.

Conventional tools, such as Homogeneous Transformation Matrix (HTM) and Denavit–Hartenberg (D–H) methods, are used to coordinate transformation from the object frame to global system [4,5]. Suh [6] introduced an error modeling method and measurement for five-axis machine tools with a rotary table. This method divided the configuration into 3 translational axes and 2 rotational axes which was studied by many scholars, but this method was too simple in location error identification. Because the accurate value of errors is important for error compensation, Rahman [7] presented an approach to implement in a processor for data including modeling and measurement of real machine tools. Zhu [8] introduced an integrated geometric error modeling, identification and compensation for CNC machine, but his work concentrated on the systematic error analysis procedure. Fan [9] raised a universal modeling method for CNC machine tools. This method developed a multi-body model and established precision machining condition equation. Uddin [10] presented a simulator of geometric errors on interference between tools and workpiece, which was used to address how errors gave impact on accuracy of

* Corresponding author at: State Key Laboratory of High-performance Complex Manufacture, Central South University, Changsha, Hunan 410083, China.
E-mail addresses: tanghao@umich.edu, tanghaocsu@csu.edu.cn (H. Tang), duanjian@csu.edu.cn (J.-a. Duan), lans@umich.edu (S. Lan), huanyis@umich.edu (H. Shui).

[1] Research area: Error transferring and precision analysis for multi-axis system.

http://dx.doi.org/10.1016/j.ijmachtools.2015.02.012
0890-6955/

Nomenclature

MAS	multi axes system
MPS	multi-axis precision stage
OPS	optoelectronic packaging system
HTM	homogeneous transformation matrix
SOV	stream of variation
X, Y, Z, U, V, W	axis in MAS
x, y, z, u, v, w	geometric error
$x^k, y^k, z^k, u^k, v^k, w^k$	kinematic error
$\alpha^l, \beta^l, \gamma^l$	location error
CS	coordinate system
P	name of CS
E	matrix of homogeneous transformation
T_0/T_n	
C	matrix of CS
M	matrix of movement
L	matrix of location error
K	matrix of kinematic error
T_0'	actual pose measured in P_0
D	matrix of deviation
SAS	six-axis stage
Y^c, Z^c	coordinate offset between two adjacent CS
$X_{axis}, Y_{axis}, Z_{axis}, U_{axis}, V_{axis}, W_{axis}$	movement of each axis

machined cone frustum in five-axis machining center. However, it was not readily adopted for other structures. Lee [11] focused on influence of individual errors on volumetric error for general five-axis machine tools configuration. However, the modeling procedure was so complicated and applications were not conclusive. Tan [12] used neural networks idea in geometric error modeling for precision system. This method was a new attempt for non-linear system, but limited in some simple configuration. Besides error modeling, how to use error model in a proper way is also important. Some scholars [13–15] used error model to expand subsequent applications, such as error compensation, error budget analysis and sensitivity analysis etc., which also contributed to error modeling and error theory for MAS.

Furthermore, there is another kind of literatures focusing on developing general error modeling method. These studied to develop approaches which were comprehensively adopted in different high-accuracy environments for MAS. Tian [16] introduced a new error modeling method based on error separation in tolerance design and error compensation. However, some geometric errors were not taken into account. In order to reduce computational effort, Lin [17] developed a new matrix summation approach in five-axis machine to break down kinematic equations into several parts with clear physical meaning. However, this method was only for five-axis machine tools, and its applicability needs to be tested with more kind of configurations. Huang [18] proposed a rigorous general and systematic procedure based on generalized Jacobian Matrix. But this method was only developed for lower mobility manipulator.

The literatures aforementioned have some limitations. Most scholars concentrate on five-axis machine tools or machining center, while MPS is adopted in many regions, such as magnet-levitation stage [2]. Furthermore, there are some differences between MPS and machine tools. Thus, a new error modeling approach based on SOV is introduced in this paper. SOV is used for measuring product quality in a complex system consists of multiple operations [19]. The deviations/variations of product quality are contributed by the errors generated in each station, and the accumulated errors transmitted from previous stations [20,21]. Unlike calculating deviations in final step, this method shows a systematic procedure about how much deviation after every station and how deviations accumulate. In this paper, for a given MAS, a new error modeling approach based on SOV theory is introduced to improve accuracy efficiently in design. Each axis is regarded as a station, and deviation after each station is propagated to next station as upstream impact. Thus, the MAS can be transformed into a multi-station system. How errors propagate and deviations accumulate can be observed to control these stations with significant variations. The new error model is systematic and easy debugging, and the error propagation process can improve the efficiency of deviation reduction.

Section 2 describes some basic concepts about geometric errors. HTM is adopted as mathematical tool to represent the pose in different coordinate system. Section 3 introduces the new error modeling approach based on SOV, and compared to conventional approach. Section 4 gives a case study and corresponding applications about error modeling for six-axis stage (SAS) which is used in controlling fiber array in OPS.

2. Geometric error definition

Generally speaking, in MAS with 6 axes, 3 translational axes are named as X, Y, Z axes, and 3 rotational axes are U, V, W axes. The geometric errors are divided into two parts: kinematic error and location error.

For a moving component, there are six kinematic errors: three translational errors (x, y, z) and three rotational errors (α, β, γ). Fig. 1 shows a translational axis moving along Y-axis and a

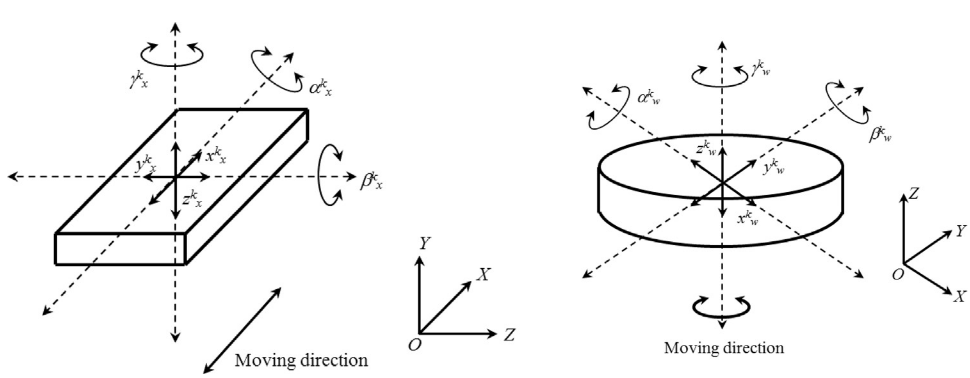

Fig. 1. Six kinematic errors in a motion axis.

Table 1
Physical meaning of kinematic errors.

Axis	Error components				
	Positioning error	Straightness error	Pitch	Yaw	Roll
X-axis	x_x^k	y_x^k, z_x^k	v_x^k	w_x^k	u_x^k
Y-axis	y_y^k	x_y^k, z_y^k	w_y^k	u_y^k	v_y^k
Z-axis	z_z^k	x_z^k, y_z^k	u_z^k	v_z^k	w_z^k
	Axial error	Radius error	Angular error	Tilt error	
U-axis	x_u^k	y_u^k, z_u^k	u_u^k	v_u^k, w_u^k	
V-axis	y_v^k	x_v^k, z_v^k	v_v^k	u_v^k, w_v^k	
W-axis	z_w^k	x_w^k, y_w^k	w_w^k	u_w^k, v_w^k	

rotational axis rotating around *Z*-axis (named *W*-axis), respectively. On the left side of figure, the positioning error is y_y^k, the two straightness errors are x_y^k, z_y^k, and pitch, yaw and roll errors are γ_y^k, α_y^k, β_y^k, respectively. On the right side, the angular error is γ_w^k, two tilt errors are α_w^k, β_w^k, and the axial error and two radius errors are z_w^k, x_w^k, y_w^k. Because error distribution of each error is different, it is important to understand the physical meaning of each error [22,23]. The superscript *k* denotes kinematic error. All errors in other directions are listed in Table 1.

Moreover, location error, named as installation errors or assembly errors, is existed between two units in installation process resulted from non-strictly orthogonality. In most cases, significant location errors are concerned as angular errors, such as verticality and parallelism.

3. New error modeling method

Assuming that an object is placed on MAS for high-accuracy positioning control, there are deviations between actual and ideal status due to geometric errors. For a given configuration of MAS, it is important to understand how error propagates from lower axis to higher axis, which is beneficial for error accumulation and sensitive error control. Thus, a comprehensive error model to connect geometric error and deviations from all directions are needed. It is also can be used for other applications besides error compensation.

In this study, SOV method is employed to solve these problems. The SOV method is widely used in engineering regions, such as modern manufacturing processes, information systems, and service processes involving multiple steps [19], and some ideas and formulas of SOV are very beneficial in error analysis, error propagation and error modeling for MAS.

For example, there is a very classic model of multi-station manufacturing system to describe how deviations accumulate by the impact of errors from upstream stations, as shown in Fig. 2.

Two corresponding formulas to describe:

$$\boldsymbol{x}_i = \boldsymbol{A}_{i-1}\boldsymbol{x}_{i-1} + \boldsymbol{B}_i\boldsymbol{u}_i + \boldsymbol{w}_i \tag{1}$$

$$\boldsymbol{y}_i = \boldsymbol{C}_i\boldsymbol{x}_i + \boldsymbol{v}_i \tag{2}$$

Here, $\boldsymbol{x}_i$ denotes the quality characteristics of product after station *i*, $\boldsymbol{u}_i$ denotes the impact by error source, $\boldsymbol{w}_i$ denotes unmodeled factors, and $\boldsymbol{v}_i$ denotes sensor noise. From this diagram, how errors give impact on product quality and how deviations accumulate can be known [20]. The SOV theory was developed by Djurjanovic [24]. Considering this theory can be used for evaluating the quality of product with multi-station process, this paper adopts SOV theory in error modeling.

The new approach based on SOV considers axis as a station, and calculates deviations after each station then adds the deviation as upstream impact into next stations until final one, as Eq. (1) shows. Because this paper only considers geometric error modeling, other irrelevant concepts like $\boldsymbol{w}_i$ and $\boldsymbol{v}_i$ are neglected in modeling procedure. Thus, each axis can be regarded as a single station, and the error model for MAS can be re-established compare to conventional method.

All concepts in error modeling of new method should be mapped to the parameters in Eq. (1). There are several essential concepts in error modeling, including kinematic errors, location errors, CS offsets, movement of each axis and the deviations after each station. According to Nebot's research work and physical meaning of each concept [21], a definition mapping of these concepts from SOV to error modeling is processed. In machining process, there are several errors impacting on quality of part, such as machine deviations, fixture deviations and errors from upstream station. Machine-induced deviations is generated when axis moves, which is similar to kinematic error; fixture-induced deviations is similar to location error; the deviations by previous CSs impact, can be regarded as upstream deviations; CS offsets and movement of each axis are constant parameters according to the distances between axes and required displacement of each axis.

So one MAS can be transferred into multi stations format (see Fig. 3):

Here, P_i denotes the CS *i*, $\boldsymbol{C}_i$ denotes the coordinate offset matrix from P_i to P_{i-1}, $\boldsymbol{L}_i$ denotes the location error matrix when CS *i* is installed on CS $i-1$, $\boldsymbol{M}_i$ denotes the movement matrix of component *i*, $\boldsymbol{K}_i$ denotes the kinematic error matrix in CS *i*, $\boldsymbol{T}_0$ denotes the pose of object in P_0 ideally, $\boldsymbol{D}_i$ denotes the deviation resulting from the previous stations P_1 to P_i, Considering that location error is generated in installation, $\boldsymbol{L}_n$ should post-multiply $\boldsymbol{C}_n$, and $\boldsymbol{K}_n$ should post-multiply $\boldsymbol{M}_n$ because it is generated by motion, and coordinate offset matrix should pre-multiply movement matrix because it is existed before moving.

For example, the deviation could be derived after station 1 as follows:

$$\boldsymbol{D}_1 = \boldsymbol{C}_1\boldsymbol{L}_1\boldsymbol{M}_1\boldsymbol{K}_1\boldsymbol{P}_0 - \boldsymbol{C}_1\boldsymbol{M}_1\boldsymbol{P}_0 \tag{3}$$

$\boldsymbol{D}_1$ denotes the deviations after station 1.

$\boldsymbol{D}_1$ could be regarded as upstream impact on station 2. $\boldsymbol{D}_2$ can be derived as follows:

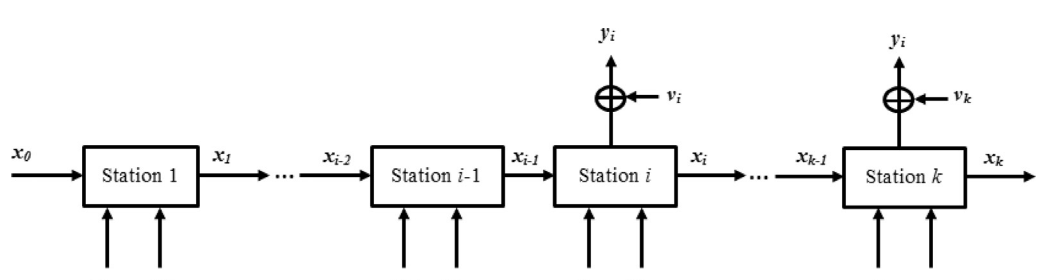

Fig. 2. Schematic of multi-station system.

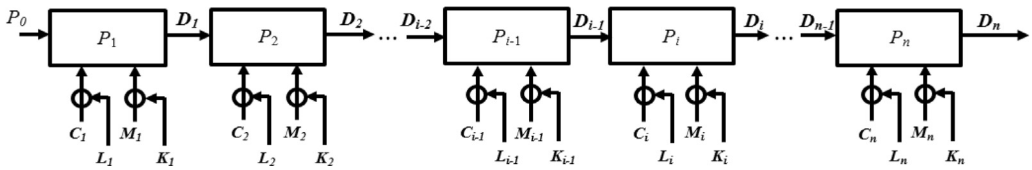

Fig. 3. Schematic of MAS described based on multi stations.

$$\boldsymbol{D}_2 = (\boldsymbol{D}_1 + \boldsymbol{P}_1)^1\boldsymbol{E}_2{}'\boldsymbol{P}_1 - {}^1\boldsymbol{E}_2\boldsymbol{P}_1 = (\boldsymbol{D}_1 + \boldsymbol{P}_1)\boldsymbol{C}_2\boldsymbol{L}_2\boldsymbol{M}_2\boldsymbol{K}_2\boldsymbol{P}_1 - \boldsymbol{C}_2\boldsymbol{M}_2\boldsymbol{P}_1 \quad (4)$$

Similarly, the deviations after each station could be derived with the same procedure:

$$\begin{aligned}\boldsymbol{D}_n &= (\boldsymbol{D}_{n-1} + \boldsymbol{P}_{n-1})^{n-1}\boldsymbol{E}_n{}'\boldsymbol{P}_{n-1} - {}^{n-1}\boldsymbol{E}_n\boldsymbol{P}_{n-1} \\ &= (\boldsymbol{D}_{n-1} + \boldsymbol{P}_{n-1})\boldsymbol{C}_n\boldsymbol{L}_n\boldsymbol{M}_n\boldsymbol{K}_n\boldsymbol{P}_{n-1} - \boldsymbol{C}_n\boldsymbol{M}_n\boldsymbol{P}_{n-1}\end{aligned} \quad (5)$$

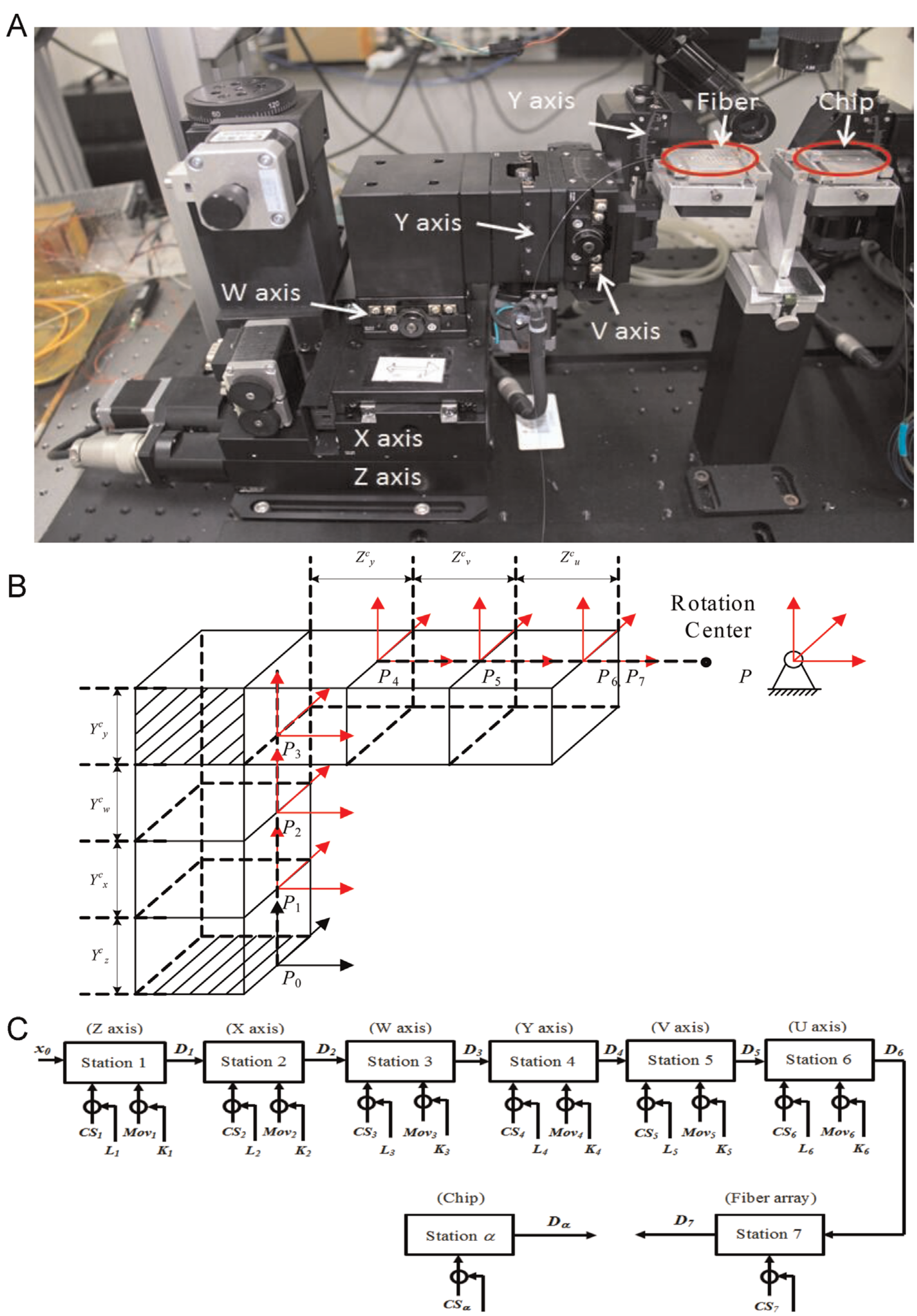

Fig. 4. A typical configuration of SAS in OPS.

4. Case study

4.1. Error modeling for six-axis stage in OPS

Fig. 4 shows a six-axis stage (SAS) controlling the pose of fiber array which is aligned with the chip in OPS. It has 3 translational axes (*X*, *Y*, *Z*) and 3 rotational axes (*U, V, W*). From low to high it is *F–Z–X–W–Y–V–U* serial configuration. In order to calculate the six directional deviations of fiber array, the new error modeling approach is employed.

Fig. 4(A) shows that SAS includes six axes motion units and fiber array which is fixed on highest component. There is a chip fixed on the ground frame.

Conventional method for establishing error model is to derive the pose of object in ground coordinate system (CS, or named global coordinate system). Kinematic errors should be considered because each component is mobile, and there is also location error between two adjacent CSs due to non-strict-orthogonality. A series of homogeneous transformation is given:

$$\boldsymbol{D}_n = \boldsymbol{T}_0{}' - \boldsymbol{T}_0 = \boldsymbol{C}_1\boldsymbol{L}_1\boldsymbol{M}_1\boldsymbol{K}_1\cdots\boldsymbol{C}_n\boldsymbol{L}_n\boldsymbol{M}_n\boldsymbol{K}_n\boldsymbol{T}_n - \boldsymbol{C}_1\boldsymbol{M}_1\cdots\boldsymbol{C}_n\boldsymbol{M}_n\cdot\boldsymbol{T}_n \tag{6}$$

$\boldsymbol{T}_0$ and $\boldsymbol{T}_0{}'$ denotes ideal and actual pose of fiber, respectively. $\boldsymbol{D}_n$ denotes the deviations in actual status measured in ground CS.

The above procedure of conventional error modeling method has some disadvantages.

1. Difficult to know error propagation procedure.
2. Difficult to debug.
3. Can only be applied for error compensation in most cases, and need to be expanded to other applications.

In Fig. 4(B), for computation convenience, all components of axes are assumed as same scale. Due to rotation center is in middle point at *X* directional sides, the *X* coordinate of origins are set in same plate with rotation center. Location errors are in consideration, so the *Y* coordinate of origins are set in installation plate. For improving computational efficiency, all coordinate systems need to be compact, then the *Z* coordinate of origins can be determined (the component's right side). Thus, all coordinate systems are setting as Fig. 4(B) above shows. There are differences between coordinate system of each axis. These differences, $Y_z{}^c$, $Y_x{}^c$, $Y_w{}^c$, $Y_y{}^c$, $Z_y{}^c$, $Z_v{}^c$, $Z_u{}^c$ should be compensated in error modeling procedure. The subscript denotes which axis it belongs to, and the superscript denotes these parameters in coordinate offset matrix.

The red CSs denote ideal CS of each axis, and fiber array CS P_7 is overlapping U-body CS P_6. P_α denotes the ideal CS of chip which is fixed on frame. Location error should be considered due to immobility. It is assumed that there is no offset between P_6 and P_7 due to small scale of fiber fixture.

Due to lower component could affect higher component, the upstream impact by lower component could be considered as previous error. Thus, after movement processing by each axis, the kinematic chain is shown in Fig. 5:

Fig. 4(C) is another type of flow chart based on SOV. After station 1 impacts, the actual pose will be transformed into Y_1, as shown in Eq. (7):

$$\begin{aligned}\boldsymbol{D}_n &= (\boldsymbol{D}_{n-1} + \boldsymbol{P}_{n-1})^{n-1}\boldsymbol{E}_n{}'\boldsymbol{P}_{n-1} - {}^{n-1}\boldsymbol{E}_n\boldsymbol{P}_{n-1}\\ &= (\boldsymbol{D}_{n-1} + \boldsymbol{P}_{n-1})\boldsymbol{C}_n\boldsymbol{L}_n\boldsymbol{M}_n\boldsymbol{K}_n\boldsymbol{P}_{n-1} - \boldsymbol{C}_n\boldsymbol{M}_n\boldsymbol{P}_{n-1}(n\\ &= 1, 2\ldots6)\end{aligned} \tag{7}$$

Considering that there are location errors in installation of fiber array and chip, $\boldsymbol{D}_7$ and $\boldsymbol{D}_\alpha$, could be derived as follows:

$$\boldsymbol{D}_7 = (\boldsymbol{D}_6 + \boldsymbol{P}_6)^6\boldsymbol{E}_7{}'\boldsymbol{P}_6 - {}^6\boldsymbol{E}_7\boldsymbol{P}_6 = (\boldsymbol{D}_6 + \boldsymbol{P}_6)\boldsymbol{L}_7\boldsymbol{P}_6 - \boldsymbol{P}_6 \tag{8}$$

$$\boldsymbol{D}_\alpha = {}^0\boldsymbol{E}_\alpha{}'\boldsymbol{P}_0 - {}^0\boldsymbol{E}_\alpha\boldsymbol{P}_0 = \boldsymbol{L}_\alpha\boldsymbol{P}_0 - \boldsymbol{P}_0 \tag{9}$$

Finally, the deviations $\boldsymbol{D}$ in alignment between fiber array and chip can be derived by subtracting $\boldsymbol{D}_\alpha$ from $\boldsymbol{D}_7$:

$$\boldsymbol{D} = \boldsymbol{D}_7 - \boldsymbol{D}_\alpha \tag{10}$$

Due to this paper concentrates on error modeling of SAS, and orientation errors cannot be affected by position error as well, the impacts by location errors in fiber array and chip are omitted.

In error modeling, the new method provides a way to observe how errors propagate and how deviations vibrate in whole procedure, which is also beneficial to understand how much percentage different errors take. These merits are helpful to decrease error in design part. The details are introduced in Section 4.2.

The new error model based on SOV calculates deviations after each station from lower to higher while has following advantages:

1. Easy to understand how errors propagate and accumulate in the whole procedure.
2. Easy to debug.
3. Comprehensive and flexible for sensitive error control.

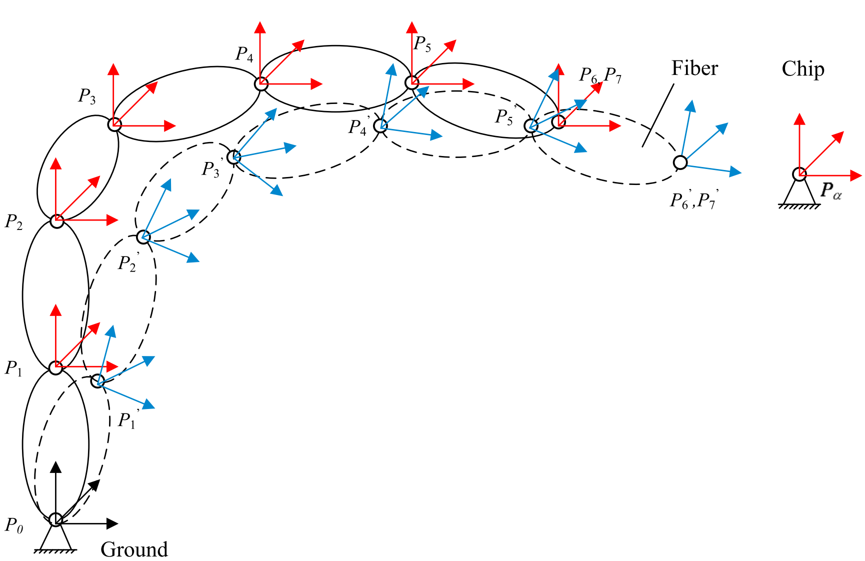

Fig. 5. Schematic of kinematic chain for SAS.

Table 2
Value of each parameter in error model.

Value	Error, offsets and movements
0.1 μm	$u_x^k, u_y^k, u_z^k, u_v^k, u_w^k, v_x^k, v_y^k, v_z^k, v_u^k, v_w^k, w_x^k, w_y^k, w_z^k, w_u^k, w_v^k$
0.5 μm	$\alpha_x^l, \alpha_u^l, \alpha_{yv}^l, \alpha_{zw}^l, \beta_y^l, \beta_v^l, \beta_{xu}^l, \beta_{zw}^l, \gamma_w^l, \gamma_z^l, \gamma_{xu}^l, \gamma_{yv}^l$
1 μm	$x_y^k, x_z^k, x_u^k, x_v^k, x_w^k, y_x^k, y_z^k, y_u^k, y_v^k, y_w^k, z_x^k, z_y^k, z_u^k, z_v^k, z_w^k$
2 μm	x_x^k, y_y^k, z_z^k
3 μm	u_u^k, v_v^k, w_w^k
1 mm	Movement of each translational axis: X_{axis}, Y_{axis}, Z_{axis}
20 mm	Offsets: $Y_z^c, Y_x^c, Y_w^c, Y_y{}^c, Z_y^c, Z_v^c, Z_u^c$
1°	Movement of each rotational axis: U_{axis}, V_{axis}, W_{axis}

Table 3
Distributions of different types of error term. Unit: μm

Translational axes		Rotational axes	
Error	Distribution	Error	Distribution
Position error	(−2.0,2.0)	Angular error	(−3.0 3.0)
Straightness error	(−1.0,1.0)	Radius error	(−1.0,1.0)
Pitch	(−0.1,0.1)	Axial error	(−1.0 1.0)
Yaw & Roll	(−0.1,0.1)	Tilt error	(−0.1,0.1)
Static error (installation accuracy)			(−0.5 0.5)

4.2. Applications

4.2.1. Sensitive stations control

In order to describe the application of the new method based on SOV theory more clearly, all offsets, movements and errors are given a value to evaluate the results (see Table 2). These values are considered as worst-case condition from the company handbook (see Table 3) [25]. The superscript l denotes location error.

The pose of fiber can be calculated expanding Eq. (7), and all values are from Table 2:

$$
\begin{aligned}
\boldsymbol{D}_1 &= \boldsymbol{C}_1\boldsymbol{L}_1\boldsymbol{M}_1\boldsymbol{K}_1\boldsymbol{P}_0 - \boldsymbol{C}_1\boldsymbol{M}_1\boldsymbol{P}_0\\
&= \begin{bmatrix} 1 & 0 & 0 & 0\\ 0 & 1 & 0 & Y_z^c\\ 0 & 0 & 1 & 0\\ 0 & 0 & 0 & 1 \end{bmatrix} \cdot \begin{bmatrix} 1 & -\gamma_z^l & 0 & 0\\ \gamma_z^l & 1 & 0 & 0\\ 0 & 0 & 1 & 0\\ 0 & 0 & 0 & 1 \end{bmatrix}\\
&\quad \cdot \begin{bmatrix} 1 & 0 & 0 & 0\\ 0 & 1 & 0 & 0\\ 0 & 0 & 1 & Z_{axis}\\ 0 & 0 & 0 & 1 \end{bmatrix}\\
&\quad \cdot \begin{bmatrix} 1 & -w_z^k & v_z^k & x_z^k\\ w_z^k & 1 & -u_z^k & y_z^k\\ -v_z^k & u_z^k & 1 & z_z^k\\ 0 & 0 & 0 & 1 \end{bmatrix} \cdot \begin{bmatrix} 1 & 0 & 0 & 0\\ 0 & 1 & 0 & 0\\ 0 & 0 & 1 & 0\\ 0 & 0 & 0 & 1 \end{bmatrix}\\
&\quad - \begin{bmatrix} 1 & 0 & 0 & 0\\ 0 & 1 & 0 & Y_z^c\\ 0 & 0 & 1 & 0\\ 0 & 0 & 0 & 1 \end{bmatrix}\\
&\quad \cdot \begin{bmatrix} 1 & 0 & 0 & 0\\ 0 & 1 & 0 & 0\\ 0 & 0 & 1 & Z_{axis}\\ 0 & 0 & 0 & 1 \end{bmatrix} \cdot \begin{bmatrix} 1 & 0 & 0 & 0\\ 0 & 1 & 0 & 0\\ 0 & 0 & 1 & 0\\ 0 & 0 & 0 & 1 \end{bmatrix}\\
&= \begin{bmatrix} 0 & -0.0006 & 0.0001 & 0.001\\ 0.0006 & 0 & -0.0001 & 0.001\\ -0.0001 & 0.0001 & 0 & 0.002\\ 0 & 0 & 0 & 0 \end{bmatrix}
\end{aligned}
\tag{11}
$$

$$
\begin{aligned}
\boldsymbol{D}_2 &= (\boldsymbol{D}_1 + \boldsymbol{P}_1)\boldsymbol{C}_2\boldsymbol{L}_2\boldsymbol{M}_2\boldsymbol{K}_2\boldsymbol{P}_1 - \boldsymbol{C}_2\boldsymbol{M}_2\boldsymbol{P}_1\\
&= \begin{bmatrix} 0 & -0.0007 & 0.0002 & -0.009\\ 0.0007 & 0 & -0.0007 & 0.0026\\ -0.0002 & 0.0007 & 0 & 0.0049\\ 0 & 0 & 0 & 0 \end{bmatrix}
\end{aligned}
\tag{12}
$$

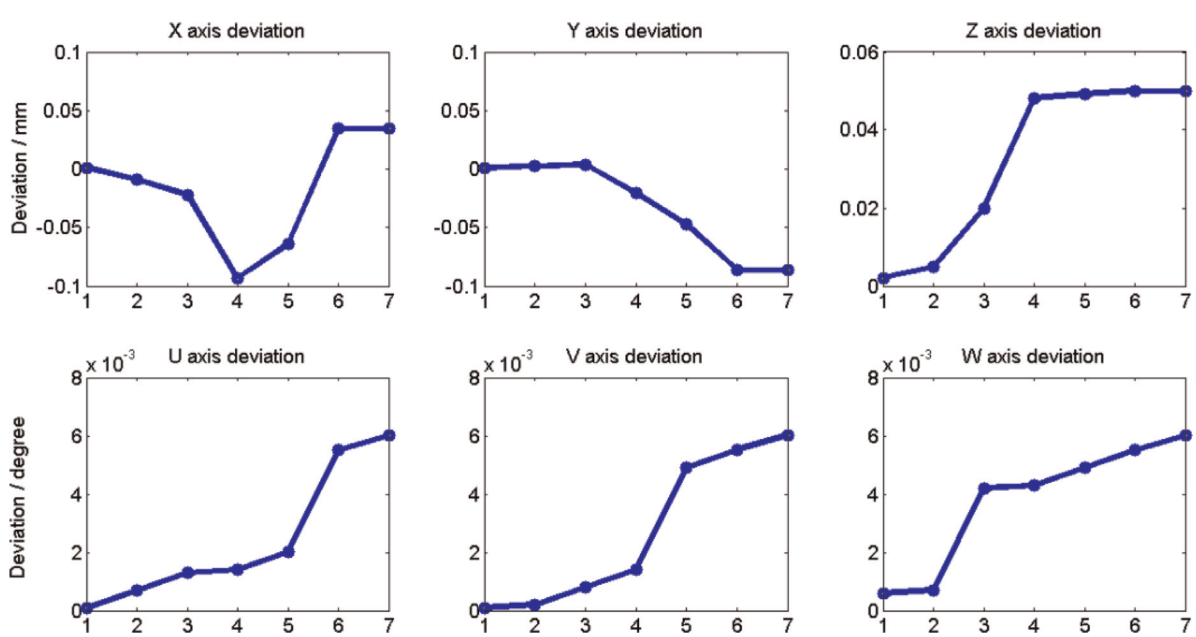

Fig. 6. Deviations after each station in SAS.

$$\boldsymbol{D}_3 = (\boldsymbol{D}_2 + \boldsymbol{P}_2)\boldsymbol{C}_3\boldsymbol{L}_3\boldsymbol{M}_3\boldsymbol{K}_3\boldsymbol{P}_2 - \boldsymbol{C}_3\boldsymbol{M}_3\boldsymbol{P}_2 = \begin{bmatrix} 0 & -0.0042 & 0.0008 & -0.022 \\ 0.0042 & 0 & -0.0013 & 0.0036 \\ -0.0008 & 0.0013 & 0 & 0.0199 \\ 0 & 0 & 0 & 0 \end{bmatrix} \tag{13}$$

$$\boldsymbol{D}_4 = (\boldsymbol{D}_3 + \boldsymbol{P}_3)\boldsymbol{C}_4\boldsymbol{L}_4\boldsymbol{M}_4\boldsymbol{K}_4\boldsymbol{P}_3 - \boldsymbol{C}_4\boldsymbol{M}_4\boldsymbol{P}_3 = \begin{bmatrix} 0 & -0.0043 & 0.0014 & -0.0932 \\ 0.0043 & 0 & -0.0014 & -0.0205 \\ -0.0014 & 0.0014 & 0 & 0.0482 \\ 0 & 0 & 0 & 0 \end{bmatrix} \tag{14}$$

$$\boldsymbol{D}_5 = (\boldsymbol{D}_4 + \boldsymbol{P}_4)\boldsymbol{C}_5\boldsymbol{L}_5\boldsymbol{M}_5\boldsymbol{K}_5\boldsymbol{P}_4 - \boldsymbol{C}_5\boldsymbol{M}_5\boldsymbol{P}_4 = \begin{bmatrix} 0 & -0.0049 & 0.0049 & -0.0642 \\ 0.0049 & 0 & -0.0020 & -0.0474 \\ -0.0049 & 0.0020 & 0 & 0.0492 \\ 0 & 0 & 0 & 0 \end{bmatrix} \tag{15}$$

$$\boldsymbol{D}_6 = (\boldsymbol{D}_5 + \boldsymbol{P}_5)\boldsymbol{C}_6\boldsymbol{L}_6\boldsymbol{M}_6\boldsymbol{K}_6\boldsymbol{P}_5 - \boldsymbol{C}_6\boldsymbol{M}_6\boldsymbol{P}_5 = \begin{bmatrix} 0 & -0.0055 & 0.0055 & 0.0349 \\ 0.0055 & 0 & -0.0055 & -0.086 \\ -0.0055 & 0.0055 & 0 & 0.05 \\ 0 & 0 & 0 & 0 \end{bmatrix} \tag{16}$$

$$\boldsymbol{D}_7 = (\boldsymbol{D}_6 + \boldsymbol{P}_6)\boldsymbol{C}_7\boldsymbol{L}_7\boldsymbol{M}_7\boldsymbol{K}_7\boldsymbol{P}_6 - \boldsymbol{C}_7\boldsymbol{M}_7\boldsymbol{P}_6 = \begin{bmatrix} 0 & -0.006 & 0.006 & 0.0349 \\ 0.006 & 0 & -0.006 & -0.086 \\ -0.006 & 0.006 & 0 & 0.05 \\ 0 & 0 & 0 & 0 \end{bmatrix} \tag{17}$$

$\boldsymbol{D}_7$ shows the pose of fiber in SAS through Eq. (17). The new error model has additional applications besides error compensation. First is sensitive error control. Due to process restriction and economic consideration, not all geometric errors can be controlled but only part of errors can be chosen. In order to make the reduction procedure more efficient, an optimal error control plan based on the new error model is presented.

Fig. 6 is drawn to understand deviation propagation. It is clear to show how deviations accumulate after every station. Station 1 to 6 stands for these axes from low to high components, *Z*–*X*–*W*–*Y*–*V*–*U*, and station 7 stands for fiber fixture.

The deviations represent the effects through previous stations impact. Taking *Z* directional deviation as an example, the value in first point is 0.001 mm, which means there is 0.001 mm deviation for the following CSs (P_2 to P_7) after *Z* axis moved. This deviation is regarded as an upstream impact to add to the rest CSs. After consider other axes movement step by step, the *Z* axis deviation of fiber is calculated. Similarly, other directional deviations of fiber can be developed as well.

It has a dramatic increase for *Z* axis deviation from station 2 to station 4 during whole process, so the errors in these stations should be paid attention instead of full procedure as other sensitivity analysis research shown [26].

Generally speaking, each error is given an initial value based on distribution in Tables 1 and 3 randomly. Extreme value is better, for considering the worst case. If we want to evaluate an error, set it as variable, and other errors are constants by the given initial value. Then the evaluated error is substituted into error model with other errors simultaneously thousands of times. Notes that the evaluated error is random every time and other errors are constant. Therefore, thousands of deviations could be obtained as well. There all 48 geometric errors in SAS (36 kinematic errors and 12 location errors, not considering location errors of fiber array and chip). All 48 errors can be analyzed as same steps. Thus, 48 groups of values for all errors and 48 corresponding groups of values for deviations are obtained. For example, if the error Z_z^k is the evaluated error, then regard it as a variable. Giving other errors a value randomly and keep them as constant. Put all values of 48 errors into model, a matrix for 6 directional deviations can be obtained. Randomize Z_z^k a great many of times and other error values are not changed, then a big amount group of results for 6 directional deviations can be derived. Similarly, other errors are evaluated through same procedure. Finally, we calculate the variance of thousands groups of each error and the variance of thousands groups of *X*, *Y*, *U* and *V* directional deviations from matrix $\boldsymbol{D}_7$ (1,4), $\boldsymbol{D}_7$ (2,4), $\boldsymbol{D}_7$ (3,2) and $\boldsymbol{D}_7$ (1,3). Obviously, if the variance of deviation is larger than the error's, it means this error is sensitive, otherwise, if smaller, it means this error is not sensitive. Thus, the error sensitive order for each direction can be derived.

Table 4
Sensitivity analysis results for *Z* axis deviation.

Description	Error terms
Sensitive	u_x^k u_y^k u_w^k u_u^k u_v^k u_z^k α_{yv}^l α_{zw}^l α_x^l α_u^l z_x^k z_y^k z_z^k z_u^k z_v^k z_w^k
Insensitive	v_x^k v_y^k v_z^k v_u^k v_v^k v_w^k β_y^l β_v^l β_{xu}^l β_{zw}^l x_x^k x_y^k x_z^k x_u^k x_v^k x_w^k y_x^k y_y^k y_z^k y_u^k y_v^k y_w^k w_x^k w_y^k w_z^k w_u^k w_v^k w_w^k γ_{xu}^l γ_{yv}^l γ_z^l γ_w^l

So there are 16 sensitive error terms for *Z* axis deviation in SAS, as Table 4 shows:

z_x^k, z_w^k, z_y^k, u_w^k, u_x^k, u_y^k, α_x^l, α_{zw}^l are sensitive errors from station 2 to 4. Thus, assuming if the 8 errors are reduced by 50%, *Z* directional deviation could decrease from 0.050 mm to 0.030 mm. Similarly, if the other 8 sensitive errors are reduced by 50%, *Z* directional deviation could decrease from 0.050 mm to 0.045 mm.

The results indicate that 50% error reduction spending on station 2 to station 4 is much more efficient than in other stations for *Z* directional deviation.

Conventional method does not have capability to solve this problem because the deviations after each station are unknown so that sensitivity analysis is only adopted in full process to reduce deviation. The proposed error model based on SOV is suitable to derive the stations with great variations by observing how deviations accumulate, and control errors in these stations to decrease deviations. It can save cost and improve efficiency compared to full process sensitive error control by conventional model.

Occasionally, there are different deviations need to be controlled. According to Doerr's [27] research, *X*, *Y*, *U* and *V* directional deviations are important in alignment between fiber array and chip. From Fig. 6, for different deviations, there are various variations existed in different sensitive stations, as listed in Table 5.

Assuming that each directional deviation is equally important, the errors with more appearances are selected as priority in sensitive stations. For example, the error u_u^k shows up in *Y* and *U* sensitive station, so it should be controlled as first step. The error u_y^k shows up in *Y* sensitive station, and also in insensitive station,

Table 5
Errors in sensitive stations in OPS.

Axis	Sensitive stations	Corresponding errors
X	3–6	x_y^k, x_u^k, x_v^k, x_w^k, v_y^k, v_u^k, v_v^k, v_w^k, w_w^k, β_y^l, β_v^l, β_{xu}^l, β_{zw}^l, γ_w^l
Y	3–6	u_y^k, u_v^k, u_u^k, u_w^k, α_u^l, α_{yv}^l, α_{zw}^l, y_y^k, y_u^k, y_v^k, y_w^k
U	5–6	u_u^k, u_v^k , α_u^l, a_{yv}^l
W	5–6	v_u^k, v_v^k, β_v^l, β_{xu}^l

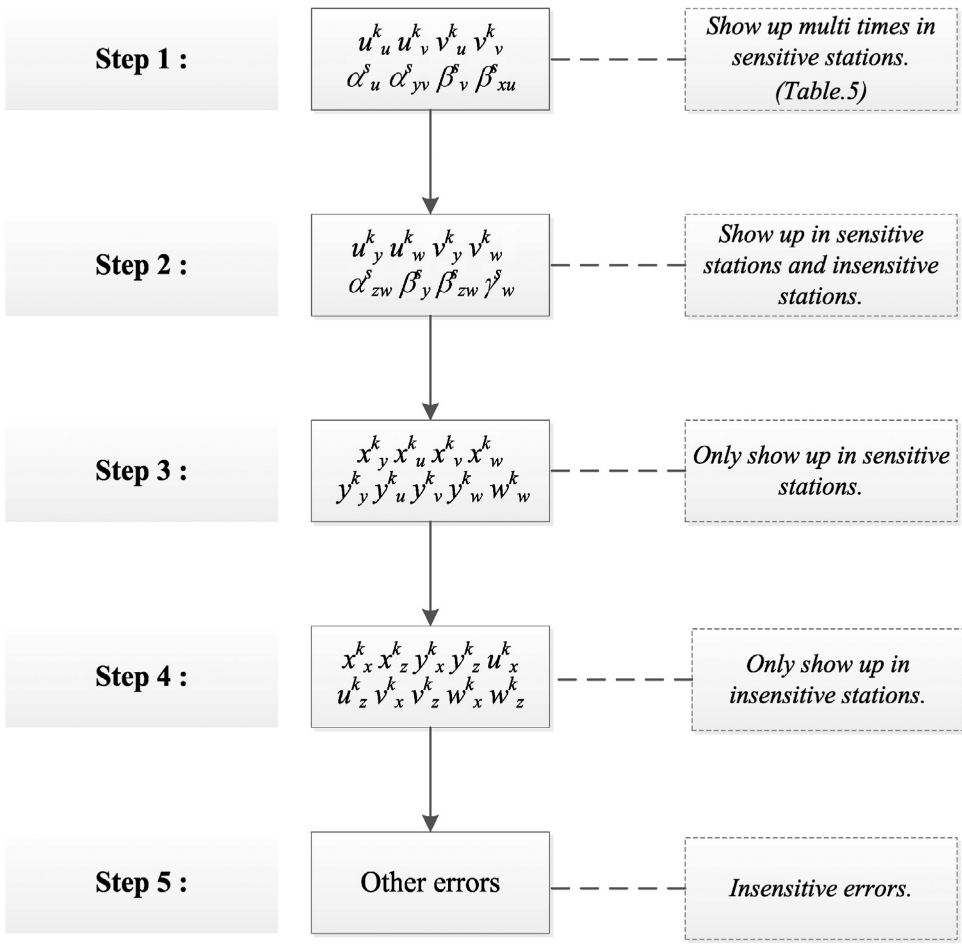

Fig. 7. Flow chart of error control order based on new error model.

so it should be controlled as second step. The full procedure is shown in Fig. 7.

From Fig. 8 there are decent deviation reduction for *X*, *U* and *V* directions after step 1. *X* directional deviation is close to 0, *U* and *V* directional deviations have 2 μrad reductions, which means the 8 sensitive errors control is more efficient. In addition, *Y* directional deviation also has 2 μm reduction.

The analyzing procedure above is an ideal situation that the values of geometric errors and offsets are given in worst case and 4 directional deviations are equally important. In other environments, not all directional deviations are in the same level, which means the weight function for different deviations should be taken into consideration.

In some cases, the configuration is giving and unchangeable,

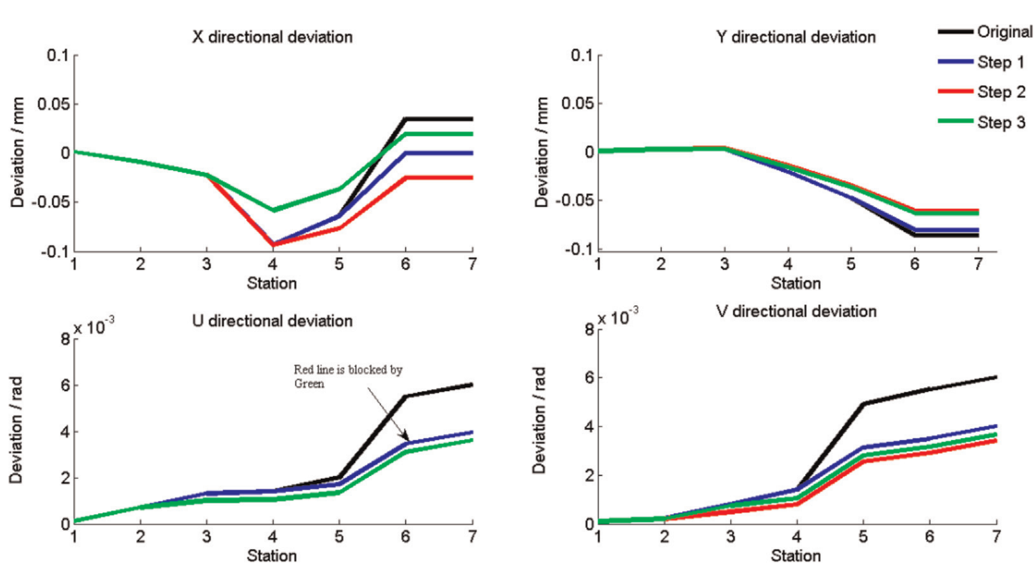

Fig. 8. Accumulation of deviation at 4 directions.

which only need to do error control to improve accuracy. The station altering gives impact on the pose of object. Thus, for different configuration selection, there is discussion in next part.

The sensitive error control based on the new error model is more efficient. Sensitivity analysis by conventional error model in full procedure is too rough to reduce deviations. The error control analysis above is developed that the errors existed in sensitive stations with comprehensive vibration are selected, which is a complement for sensitivity analysis for conventional approach.

4.2.2. Optimal configuration selection

Another application for new error model is optimal configuration selection. How to choose an optimal configuration for MPS in OPS to keep high-accuracy is crucial. There are some clauses need to be followed in OPS: *X*, *Y*, *U* and *V* directional deviations are more important in alignment between fiber and chip [27]. The translational axis does not affect rotational axis, while rotational axis affects translational axis. So translational axis is set as lower component in most case, and rotational axis is set as higher component. The three configurations listed below are typical structure from some enterprises [25,28].

Conventional approach can be used to establish error model for current configuration, but difficult to understand why this type is selected. For example, in a CNC machine, it is important to know which position the tool tip is, as conventional error model does. If there is a threshold for tool tip that the pose of tool tip should be controlled in a certain range, like over-machining, it is necessary to understand how error propagates and how deviations accumulate. By observing the deviations after each station, a proper configuration is selected by the new error model.

As mentioned in Section 4, for a SAS used in OPS, the important deviations are *X*, *Y*, *U* and *V* direction. The typical configuration from low axis to high is *Z–X–W–Y–V–U*. Besides, there are two configurations *Y–W–V–U–Z–X* and *X–Y–U–W–V–Z*, which are adopted in other environments in optoelectronic industry [28]. Thus, a comparison is proposed to select an optimal configuration for OPS requirements with the proposed error model.

Similarly, the deviations of the three configurations can be calculated following the same procedure.

From Fig. 9 the first (*Z–X–W–Y–V–U*) has a less deviation at *X* directional deviation, while the second (*Y–W–V–U–Z–X*) has a less deviation at *Y* directional deviation, and the *U* and *V* directional deviations are same in these three configurations. Thus, it is difficult to select an optimal one for SAS in OPS.

Another concept is used to choose among the three configurations. The square between curves of deviation and 0 can be regarded to evaluate the accuracy in whole process. Traditional concept for deviation is 1-D. In the new error model, the deviation can be considered as a 2-D parameter related to station also. The square in Fig. 10 does not have an actual physical meaning. It is only used for comparison among different configurations. Similarly, the square of the configuration *Y–W–V–U–Z–X* can be calculated by same procedure.

From Fig. 10 that compared to the second configuration (*Y–W–V–U–Z–X*), the first (*Z–W–X–Y–U–V*) has smaller square in *X* and *U* directional deviations, almost equal in *V* directional deviation, and bigger in *Y* directional deviation. Actually, in OPS industry, the first one is widely used.

It is possible that there is a great spike or gap in deviation during the whole accumulation procedure. Sometimes even though the final deviation is good, the deviation is beyond given threshold in one station, which is unacceptable. Based on the new error modeling approach, the deviation status can be observed throughout the procedure, which is beneficial for configuration selection.

5. Conclusions

In this paper, a new geometric error modeling approach based on SOV for MAS is introduced. It can evaluate intermediate deviations by regarding axes as successive stations. Instead of calculating deviations in final step by conventional method, the proposed error model calculates deviations after each station, and added into next station as upstream impact. So it is easy to know the deviations gradually, which can provide informative guide for designers and engineers. The new error modeling approach based on SOV the following advantages:

1. It can easily understand how errors propagate and how deviations accumulate. It is important to observe the accumulation procedure to debug in design part.
2. It is systematic and comprehensive. The new error modeling procedure is flexible with MAS configuration changing, when

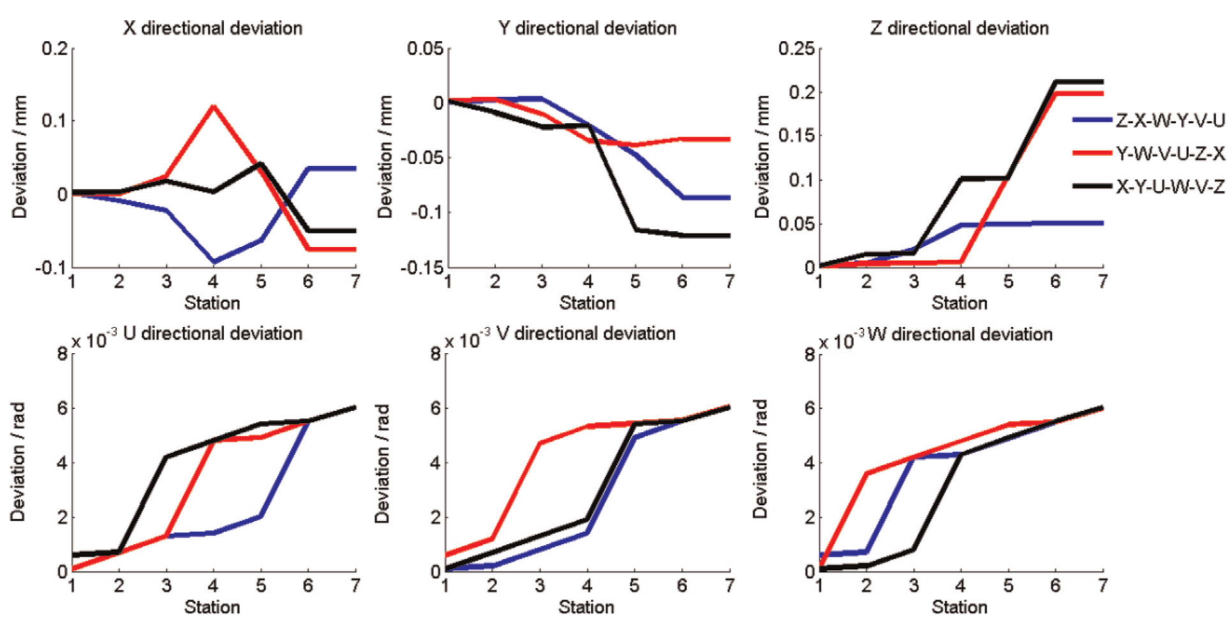

Fig. 9. Propagation of 6 directional deviations in 3 different configurations.

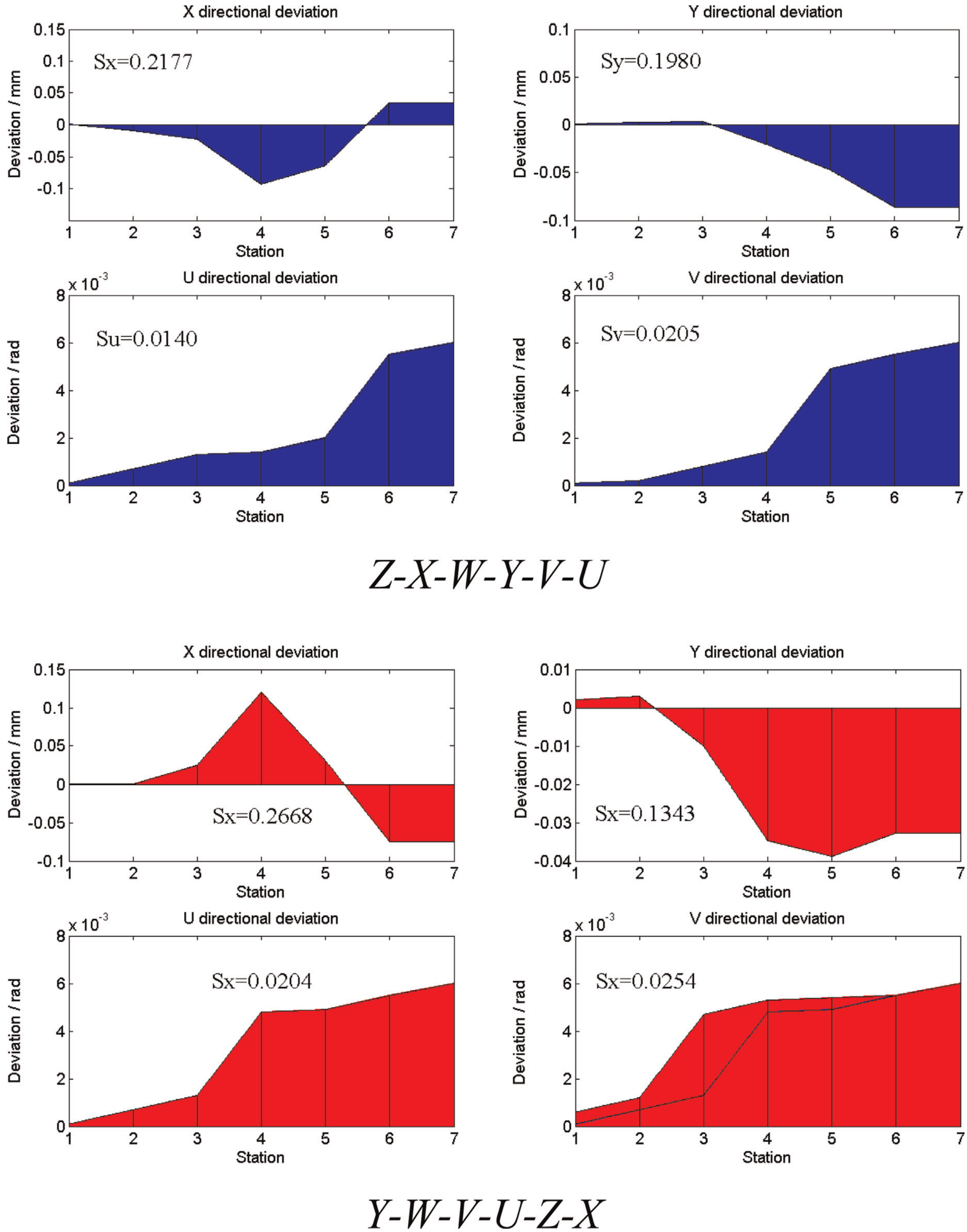

Fig. 10. Comparison between two configurations.

adding or deleting corresponding stations.

3. Beneficial in sensitive error control. The new error model can find sensitive station with great variation, so an efficient error reduction order is developed, and the analyzing procedure is important for MAS in other environments to improve accuracy. Furthermore, through comparing the deviations of different configurations based on the new error model by the concept 'square', an optimal configuration of SAS in OPS is selected.

Acknowledgments

This research is supported by the National Natural Science Foundation of China (Grant nos. 51075402 and 50975293), the National High-Tech R&D Program of China (Grant no. 2012AA040406), and the Research Fund for the Doctoral Program of Higher Education of China (Grant no. 20110162130004)

References

[1] M.A. Mannan, R. Ramesh, A.N. Poo, Error compensation for machine tools – a review. Part I: geometric, cutting-force induced and fixture-dependent errors, Int. J. Mach. Tools Manuf. 40 (2000) 1235–1256.

[2] S.K. Kuo, X. Shan, C.H. Menq, Large travel ultra-precision x-y-θ motion control of a magnetic-suspension stage, IEEE/ASME Trans. Mechatron. 8 (2003) 334–341.

[3] M.M. Prado, A.F. Gasca, G.H. Ruiz, et al., Multi-axis motion controller for robotic applications implemented on an FPGA, Int. J. Adv. Manuf. Technol. 67 (2013) 2367–2376.

[4] V. Kiridena, P.M. Ferreira, Mapping of the effects of positioning errors on the volumetric accuracy of five-axis CNC machine tools, Int. J. Adv. Manuf. Technol. 33 (3) (1993) 417–437.

[5] A.C. Okafor, Y.M. Ertekin, Derivation of machine tool error models and error compensation procedure for three axes vertical machining center using rigid body kinematics, Int. J. Adv. Manuf. Technol. 40 (8) (2000) 1199–1213.

[6] S.H. Suh, E.S. Lee, S.Y. Jung, Error modeling and measurement for the rotary table of five-axis machine tools, Int. J. Adv. Manuf. Technol. 14 (1998) 656–663.

[7] M. Rahman, J. Heikkala, K. Lappalainen, Modeling, measurement and error compensation of multi-axis machine tools. Part I: theory, Int. J. Mach. Tools Manuf. 40 (2000) 1535–1546.

[8] S.W. Zhu, G.F. Ding, S.F. Qin, et al., Integrated geometric error modeling, identification and compensation of CNC machine tools, Int. J. Mach. Tools Manuf. 52 (2012) 24–29.

[9] J.W. Fan, J.L. Guan, W.C. Wang, et al., A universal modeling method for enhancement the volumetric accuracy of CNC machine tools, J. Mater. Process. Technol. 129 (2002) 624–628.

[10] M.S. Uddin, S. Ibaraki, A. Matsubara, et al., Prediction and compensation of machining geometric errors of five-axis machining centers with kinematic errors, Precis. Eng. 33 (2009) 194–201.

[11] R.S. Lee, Y.H. Lin, Applying bidirectional kinematics to assembly error analysis for five-axis machine tools with general orthogonal configuration, Int. J. Adv. Manuf. Technol. 62 (2011) 1261–1272.

[12] K.K. Tan, S.N. Huang, S.Y. Lim, et al., Geometric error modeling and compensation using neural networks, IEEE Trans. Syst. Man Cybern. 36 (2006) 1261–1272.

[13] X. Cheng, X., L. Li, Y.M. Huang, et al., . Study on the error distribution and key parameters for a desktop multi-axis micro milling machine tool, Int. J. Adv. Manuf. Technol. 67 (2013) 2521–2527.

[14] P. Majda, Modeling of geometric errors of linear guideway and their influence on joint kinematic error in machine tools, Precis. Eng. 36 (2012) 369–378.

[15] B. Zi, H.F. Ding, X. Wu, et al., Error modeling and sensitivity analysis of a hybrid-driven based cable parallel manipulator, Precis. Eng. 38 (2014) 197–211.

[16] W.J. Tian, W.G. Gao, D.W. Zhang, et al., A general approach for error modeling of machine tools, Int. J. Mach. Tools Manuf. 79 (2014) 17–23.

[17] Y. Lin, Y. Shen, Modeling of five-axis machine tools metrology models using the matrix summation approach, Int. J. Adv. Manuf. Technol. 21 (2003) 243–248.

[18] T. Huang, H.T. Liu, D.G. Chetwynd, Generalized Jacobian analysis of lower mobility manipulators, Mech. Mach. Theory 46 (2011) 831–844.

[19] J.J. Shi, Stream of Variation Modeling and Analysis for Multistage Manufacturing Processes, CRC Press, Boca Raton, FL, 2007.

[20] J.J. Shi, S.Y. Zhou, Quality control and improvement for multistage systems: a survey, IIE Trans. 41 (2009) 744–753.

[21] J.V. Abellan-Nebot, F.R. Subiron, J.S. Mira, Manufacturing variation models in multi-station machining systems, Int. J. Adv. Manuf. Technol. 64 (2013) 63–83.

[22] ISO 230-1, Test Code for Machine Tools. Part 1. Geometric Accuracy of Machines Operating Under No-Load or Finishing Conditions, ISO, Geneva, 1996.

[23] ISO 230-7, Test Code for Machine Tools. Part 7. Geometric Accuracy of Axes of Rotation, ISO, Geneva, 2006.

[24] D. Djurdjanovic, J. Ni, Dimensional errors of fixtures, and measurement datum features in the stream of variation modeling in machining, J. Manuf. Sci. Eng. Trans. ASME 125 (2003) 716–730.

[25] Suruga Seiki Corporation. Suruga Fiber Alignment Information: Alignment System 〈http://eng.surugaseiki.com/alignment〉.

[26] H. Tang, J. Duan, S.H. Lan, An optimized error modeling approach based on error sensitivity analysis for six-axis stage in Optoelectronic packaging system. Int. J. Precis. Eng. Manuf. (submitted for publication).

[27] C.R. Doerr, Beam propagation method tailored for step-index waveguides, IEEE Photon. Technol. Lett. 13 (2) (2001) 130–132.

[28] Newport Corporation. Newport Fiber Alignment Stages Information: Ultra-Align Precision Fiber Optic Alignment Stages〈http://www.newport.com/Fiber-Alignment-Stages〉.